FISEVIER

Contents lists available at ScienceDirect

# Surface & Coatings Technology

journal homepage: www.elsevier.com/locate/surfcoat



# Tribological performance of plasma sprayed Al<sub>2</sub>O<sub>3</sub>–Y<sub>2</sub>O<sub>3</sub> composite coatings



Jian Rong a,b, Kai Yang a,\*, Huayu Zhao a, Chenguang Liu a, Yin Zhuang a, Shunyan Tao a,\*

- <sup>a</sup> Key Laboratory of Inorganic Coating Materials CAS, Shanghai Institute of Ceramics, Chinese Academy of Sciences, Shanghai 201899, PR China
- <sup>b</sup> University of Chinese Academy of Sciences, Beijing 100039, PR China

#### ARTICLE INFO

Article history: Received 31 December 2015 Revised 25 May 2016 Accepted in revised form 21 June 2016 Available online 23 June 2016

Keywords: Plasma spraying Alumina Yttria Friction and wear

#### ABSTRACT

In the present study,  $Al_2O_3$  and  $Al_2O_3-Y_2O_3$  composite coatings were deposited by atmospheric plasma spraying. The microstructure, hardness, thermal conductivity and dry sliding wear behavior of the coatings were examined. The results showed that the mass ratio of  $\alpha$ - $Al_2O_3/\gamma$ - $Al_2O_3$  in as-sprayed  $Al_2O_3$  coating was 0.08. However, the corresponding value in  $Al_2O_3-Y_2O_3$  composite coating was 0.53. This exhibits salient influence on the stabilization of  $\alpha$ - $Al_2O_3$ . The addition of  $Y_2O_3$  was beneficial to improve the thermal conductivity of the composite coating. In addition,  $Al_2O_3-Y_2O_3$  composite coating/graphite pairs possess more stable friction coefficients, which may be related to the formation of more effective and stable graphite transferred film on the surface of the coating subjected to abrasion. Further, the wear resistance of  $Al_2O_3-Y_2O_3$  composite coatings was superior to that of  $Al_2O_3$  coatings.

© 2016 Elsevier B.V. All rights reserved.

#### 1. Introduction

Thermal sprayed oxide ceramic coatings, as an appropriate candidate, have been widely used in industries, to offer wear and corrosion protection, erosion resistance and thermal insulation [1–4]. A typical representative, possessing high strength, high hardness and good oxidation resistance, alumina as are widespread applied in bearings, valves, plungers, pump seals, engine components, vacuum tube envelops, rocket nozzles, railroad components, etc. [5]. Al<sub>2</sub>O<sub>3</sub> coatings, by virtue of their inherent attrition and corrosive resistance, excellent dielectric and thermal shock resistance have attracted attention for special surface protection of metallic components operating under severe running conditions [6,7].

Rare earth elements are extensively used in surface engineering as additives to refinement of microstructure owing to its high chemical activity. Studies performed by Zhang, et al. [8] have found that appropriate addition of La<sub>2</sub>O<sub>3</sub> or CeO<sub>2</sub> has the effects of homogenization of elements, improvement of hardness and wear resistance in supersonic plasma sprayed (SPS) CoCrW coatings. Meanwhile, La<sub>2</sub>O<sub>3</sub> or CeO<sub>2</sub> with hexagonal layer structure has better lubrication function, and stable chemical properties up to 973 K [8]. Similar results were also reported in Nibased alloy [9] and Fe-based alloy [10] coatings prepared by laser cladding, electrospark deposition [11] and flame spraying [12]. At most cases, rare earth elements with less content are acted as seasoning, distributed irregularly at the boundary, making a dragging effect on the movement of grain boundary, thus facilitated to refine the

E-mail addresses: kaiyang@mail.sic.ac.cn (K. Yang), kaiyang@mail.sic.ac.cn (S. Tao).

microstructure. However, a clear correlation between the effect of rare earth oxides on  $Al_2O_3$  coating and its link with tribological performance has so far eluded researchers. In the present study, yttria was introduced into alumina coating, which can serve not only as rare earth oxide but also as reactant under high temperature, so as to offer an experimental basis to expand a promising applied field of rare earth.

### 2. Experimental procedures

#### 2.1. Materials and preparation

Stainless steel (1Cr18Ni9Ti) plates with the dimension of  $16 \text{ mm} \times 27 \text{ mm} \times 1.3 \text{ mm}$  were used as substrates, which were sand blasted using corundum, followed by ultrasonically cleaning in ethanol before the spraying process. Plasma spraying was performed by means of a MultiCoat™ spraying system equipped with a F4MB-XL plasma gun (Sulzer Metco AG, Switzerland). A mixture of Ar and H2 was used as plasma gas. NiCr powder was chosen to deposit the bond coat. Commercially available Al<sub>2</sub>O<sub>3</sub> and Y<sub>2</sub>O<sub>3</sub> powders were used as feedstock for ceramic coatings. Al<sub>2</sub>O<sub>3</sub> were fused and crushed powders, showing angular and irregular morphology while, Y<sub>2</sub>O<sub>3</sub> were agglomerated and sintered powders, showing spherical shape. The Al<sub>2</sub>O<sub>3</sub> and Y<sub>2</sub>O<sub>3</sub> powders were fed into a jar proportionally and mechanical mixed without grinding balls on a ball mill for 120 h in order to get evenly dispersed feedstock and then sprayed for the preparation of composite coatings. The morphologies of the two single and mixed powders were presented in Fig. 1. The average sizes ( $D_{50}$ ) of  $Al_2O_3$  and  $Y_2O_3$  feedstock are 20.2  $\mu m$ and 39.0 µm, respectively. The corresponding particle size distributions (shown in Fig. 2) were acquired using a Microtrac S3500 Particle Size

Corresponding authors.

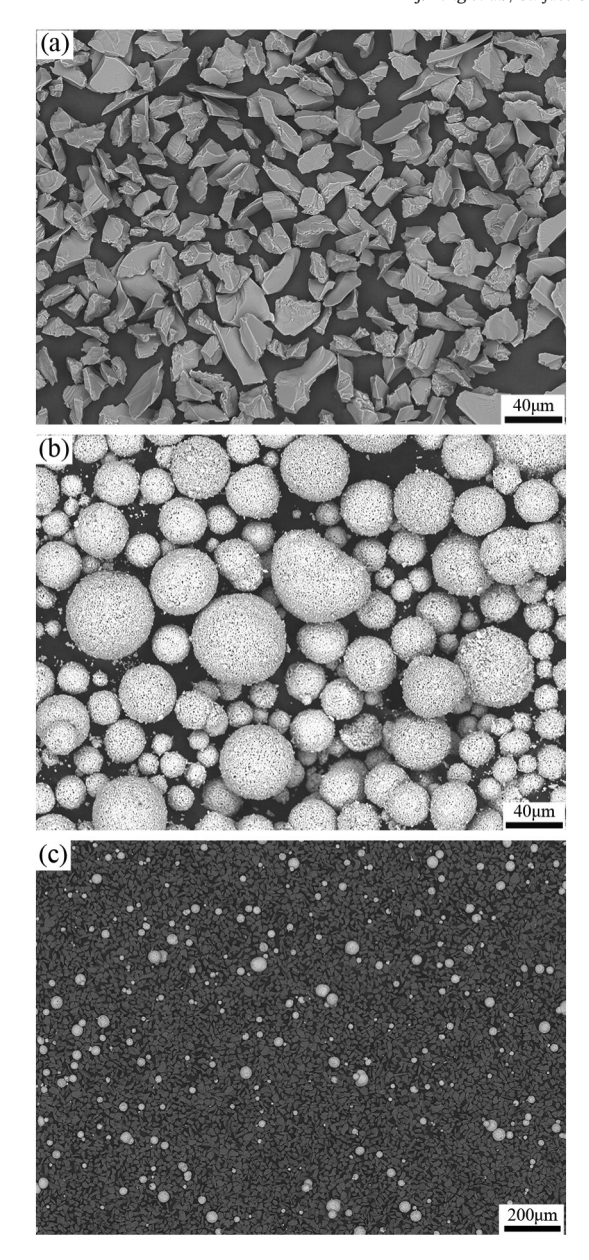


Fig. 1. Morphologies of feedstock powders: (a) Al<sub>2</sub>O<sub>3</sub>, (b) Y<sub>2</sub>O<sub>3</sub>, (c) Al<sub>2</sub>O<sub>3</sub>–Y<sub>2</sub>O<sub>3</sub>.

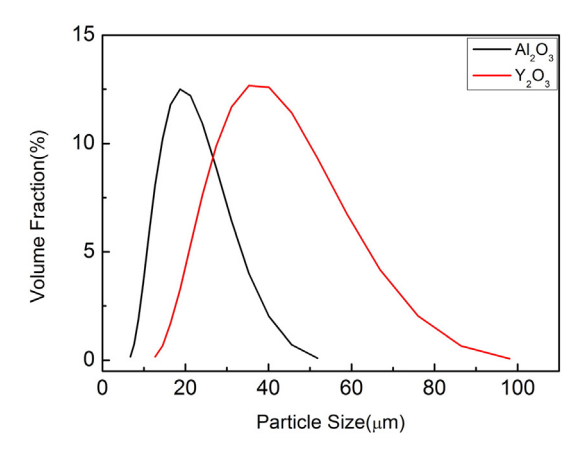


Fig. 2. Particle size distributions of original powders.

Analyser (Nikkiso, Japan). Taking the relatively low eutectic point into consideration, the mole ratio of  $Al_2O_3$  and  $Y_2O_3$  was taken as 82:18 [13], thus the mixed powders have more ability to react with each other in the plasma flame. Pure  $Al_2O_3$  coatings were also deposited for comparison. Listed in Table 1 is the plasma spraying parameters.

#### 2.2. Coating characterization

The phase compositions of the powders and corresponding coatings were determined by X-ray diffraction (XRD) using a Rigaku D/Max2550 Diffractometer with nickel-filtered Cu K $\alpha$  radiation ( $\lambda=0.15406$  nm). The XRD data were collected in the  $2\theta$  range from  $10^\circ$  to  $90^\circ$  at a scanning speed of  $1^\circ$  min $^{-1}$ . A Hitachi TM3000 scanning electron microscope (SEM) equipped with energy disperse spectroscopy (EDS) was carried out for imaging the powders, the microstructure of the coatings, and the wear tracks. Image analysis (IA) method was employed to estimate the porosity of the coatings. Ten arbitrarily selected SEM micrographs (magnification of  $1000\times$ ) were quantified for each coating sample.

Information of the thermal diffusivity ( $\alpha$ ), together with the specific heat ( $c_p$ ) and bulk density ( $\rho$ ), allows the determination of thermal conductivity ( $\lambda$ ) from [17].

$$\alpha = \frac{1.38L^2}{\pi^2 t_{1/2}} \tag{1}$$

$$\lambda = \alpha c_p \rho \tag{2}$$

where  $t_{1/2}$  is the time required for the rear face of the coating sample to reach the half-maximum of the temperature rise and L is the specimen thickness. Pure ceramic coatings without bond coating were deposited on graphite substrate (dimension  $\Phi$ 30 mm  $\times$  3.5 mm) for thermal diffusivity measurement. Coating specimens were peeled off from the graphite substrate and further machined to measure the thermal diffusivity using the laser-flash technique [14]. Specific heat capacity measurements were carried out using a modulated differential scanning calorimeter (Diamond DSC, PE, USA).

Vickers microhardness was measured with an Instron Wilson Wolpert Tukon 2100B Hardness Tester (200 g load for 10 s) on the polished cross-section of as-sprayed coatings. Considering the dependence of microhardness on the specific location within through-thickness direction [15], the indentations were executed near the centerline on the cross-section of the coatings. The hardness was obtained from the mean of the ten readings.

#### 2.3. Tribological testing

Friction and wear tests were carried out on a MM-200 (Shanghai Research Institute of Materials, China) tribological tester using a block-on-ring layout at room temperature. The schematic illustration of wear tester is shown in Fig. 3. The dimensions of stainless steel ring and graphite block were  $\Phi_{outer}$  40 mm  $\times$   $\Phi_{inner}$  16 mm  $\times$  10 mm and 30 mm  $\times$  7 mm  $\times$  6 mm, respectively. The thickness of top ceramic coatings on the stainless steel ring surfaces after grinding and polishing were about 450  $\mu$ m. Before the wear testing, the surface roughness (Ra), determined by a HOMMEL-ETAMIC T8000 roughness tester

**Table 1**Plasma spraying parameters used in the current work.

Parameters	Value	Unit
Arc current	650	A
Primary plasma gas (Ar)	40	splm
Secondary plasma gas (H <sub>2</sub> )	10	splm
Carrier gas (Ar)	3.5	splm
Powder feed rate	35	g min <sup>-1</sup>
Spray distance	110	mm

## Download English Version:

# https://daneshyari.com/en/article/8025318

Download Persian Version:

https://daneshyari.com/article/8025318

<u>Daneshyari.com</u>